THE JOURNAL OF PHYSICAL CHEMISTRY Letters

Letter

pubs.acs.org/JPCL

Revealing the Electronic and Molecular Structure of Randomly Oriented Molecules by Polarized Two-Photon Spectroscopy

Marcelo G. Vivas,*[,†] Daniel L. Silva,[‡] Leonardo De Boni,[†] Yann Bretonniere,[§] Chantal Andraud,[§] Florence Laibe-Darbour,[⊥] J.-C. Mulatier,[⊥] Robert Zaleśny,[#] Wojciech Bartkowiak,[#] Sylvio Canuto,[‡] and Cleber R. Mendonca*[,†]

[†]Instituto de Física de São Carlos, Universidade de São Paulo, Caixa Postal 369, 13560-970 São Carlos, SP, Brazil

[‡]Instituto de Física, Universidade de São Paulo, CP 66318, 05314-970 São Paulo, SP, Brazil

[§]CNRS, Université Lyon I, ENS-Lyon, 46 allée d'Itale, 69364 Lyon, France

[⊥]Laboratoire de Chimie, CNRS UR 5182, ENS de Lyon, Université Lyon I, 46 allée d'Italie, 69364 Lyon cedex 07, France

[#]Theoretical Chemistry Group, Institute of Physical and Theoretical Chemistry, Wroclaw University of Technology, Wybrzeze Wyspianskiego 27, 50-370 Wroclaw, Poland

Supporting Information

ABSTRACT: In this Letter, we explored the use of polarized two-photon absorption (2PA) spectroscopy, which brings additional information when compared to methods that do not use polarization control, to investigate the electronic and molecular structure of two chromophores (**FD43** and **FD48**) based on phenylacetylene moieties. The results were analyzed using quantum chemical calculations of the two-photon transition strengths for circularly and linearly polarized light, provided by the response function formalism. On the basis of these data, it was possible to distinguish and identify the excited electronic states responsible for the lowest-energy 2PA-allowed band in both chromophores. By modeling the 2PA circular−linear dichroism, within the sum-over-essential states approach, we obtained the relative orientation between the dipole moments that are associated with the molecular structure of the chromophores in solution. This result allowed to correlate the V-shape structure of the **FD48** chromophore and the quantum-interference-modulated 2PA strength.

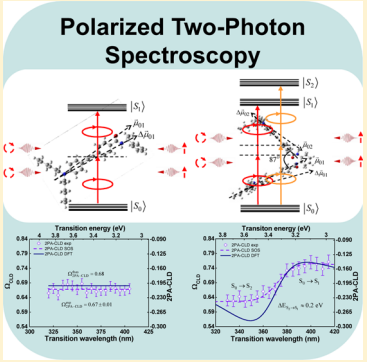

SECTION: Spectroscopy, Photochemistry, and Excited States

Due to its great technological appeal, in the past few years, two-photon absorption (2PA) spectroscopy of organic molecules has been the target of several studies, from the development of new two-photon absorbing materials to the understanding of the 2PA at a molecular level.[1−18] According to quantum mechanical perturbation theory, the probability of the 2PA to occur in the case of molecular systems depends essentially on the excitation energy, transition dipole moments from ground to excited states ($\vec{\mu}_{g\rightarrow e}$), those between excited states ($\vec{\mu}_{e\rightarrow e'}$), permanent dipole moment changes ($\Delta\vec{\mu}$), and the polarization state of ultrashort laser pulse.[19,20] While there is a great deal of attention given to optimizing the molecular structure of organic compounds, aiming at increasing their hyperpolarizabilities, polarization effects on the 2PA are underexplored.[21,22] However, this subject may offer opportunities to study in detail the electronic and molecular structure of randomly oriented chromophores, such as, for instance, that in solutions.[23−26]

The potential of polarization-dependent 2PA spectroscopy for identifying the nature of the excited states and molecular structure of randomly oriented chromophores was first shown, theoretically, by Monson and McClain[27] in 1971. Even so, until now, only some papers, particularly theoretical works, have focused on the light polarization effect on the 2PA in order to gather information about the excited states' symmetry and 3D structure of molecules in solution. For example, Tinoco[25] and Power[28] analytically showed, using the second-order perturbation theory, the two-photon absorption circular dichroism (2PA-CD) of chiral samples. Such a methodology allows, in chiral samples, exploration of optical effects beyond the electric dipole approximation. Wanapun,[29] Olesiak-Bańska,[30] and Mojzisova[31] showed the potential of the polarized two-photon spectroscopy to investigate complex molecular structures such as protein secondary structure and organization of liquid-crystalline DNA. Theisen and co-workers[24] used polarization-resolved pump−probe to determine the 3D orientation of transition dipole moments and to identify configurational isomers. More recently, Diaz et al.[32] theoretically studied the effect of the π-electron delocalization curvature on the two-photon circular dichroism of molecules with axial chirality. In summary, the polarized 2PA spectroscopy is capable of

Received: April 1, 2013
Accepted: May 1, 2013
Published: May 1, 2013

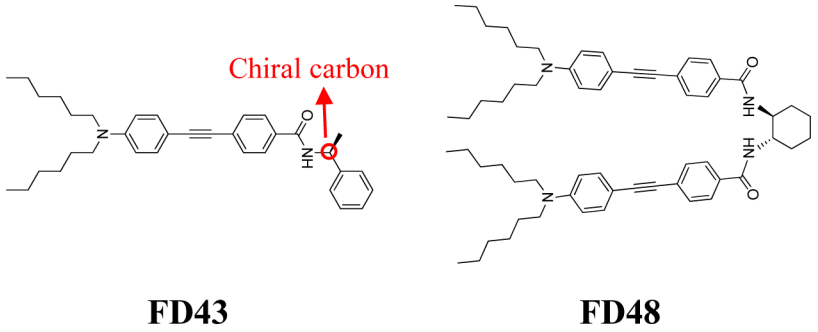

Figure 1. Structures of the phenylacetylene-based chiral molecules studied (**FD43** and **FD48**).

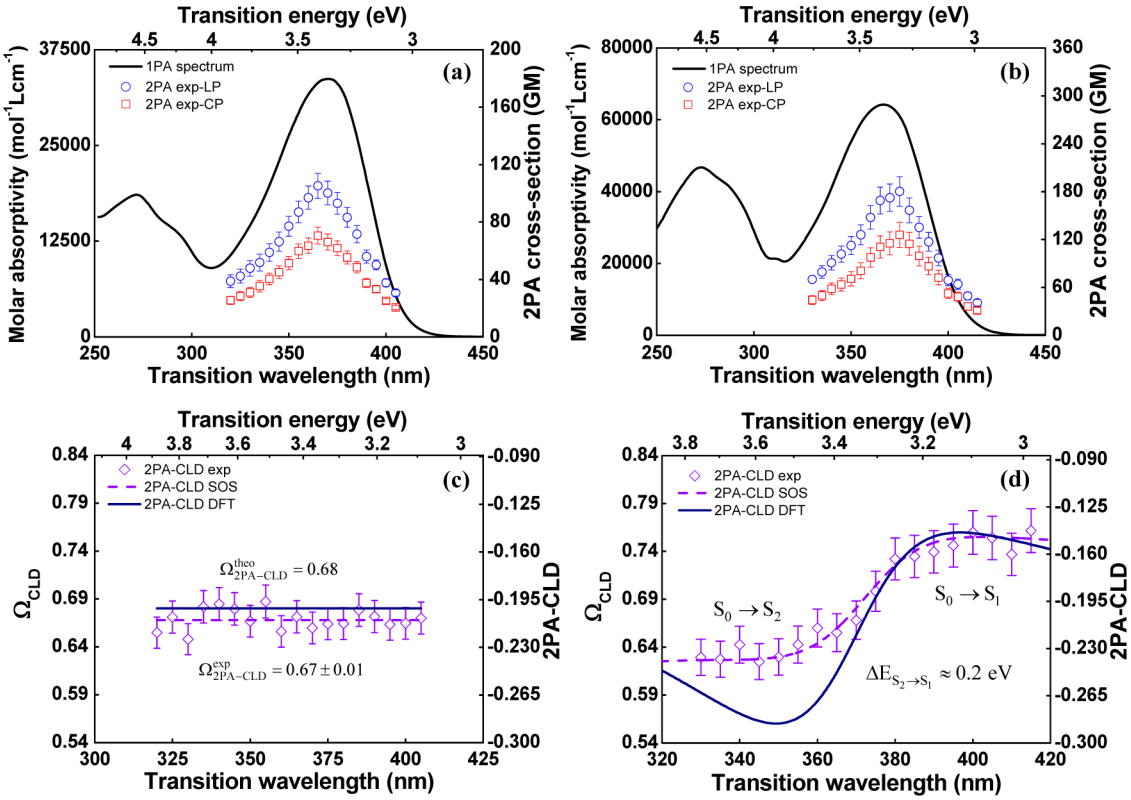

Figure 2. Experimental 1PA (solid black lines) and 2PA (circles for linear polarization and squares for circular polarization) spectra of (a) **FD43** and (b) **FD48**. Experimental (diamonds) and simulated (solid lines) 2PA-CLD spectra of (c) **FD43** and (d) **FD48**. Dashed lines show the fit employing the SOS approach.

providing information about the angle between dipole moments,[33,34] the symmetry of excited states,[23,35] and the 3D molecular structure of randomly oriented molecules,[24] and in the case of chiral samples, it allows one to obtain information about the magnetic dipole and electric quadrupole moments.[25,28,36] On the other hand, from the experimental point of view, 2PA spectroscopy of isotropic liquids has been routinely performed using linearly polarized light. Therefore, experimental studies about the polarization effects on the 2PA are of fundamental importance to gain a deeper understanding of the photophysical properties of organic molecules.

In what follows, we shall analyze the electronic and molecular structure of two chiral π-conjugated molecules with linear ((*S*)-4-((4-(dihexylamino)phenyl)ethynyl)-*N*-(1-phenylethyl) benzamide, **FD43**) and V-shape (*N*,*N*′-((1*S*,2*S*)-cyclohexane-1,2-diyl)bis(4-((4-(dihexylamino)phenyl)ethynyl)benzamide), **FD48**) molecular structures containing phenylacetylene moieties. Chiral π-conjugated molecules, as the ones studied here, are of great interest in physical chemistry and photonics because they allow exploration of distinct effects of light–matter interactions,[25,28] enable considerable improvement in the second-order nonlinear optical response,[37] and have latent application in new technologies. For example, the inherent three-dimensional character of the chirality and the high hyperpolarizabilities of conjugated systems together provide versatile chemical structures for fabrication of light-emitting diodes, fluorescent sensors, photovoltaic cells, field effect transistors, photodiodes, and so on.[38]

The discussion here is based on the 2PA circular–linear dichroism (2PA-CLD) experimental data and further supported by the results of electronic structure calculations. 2PA-CLD is a third-order nonlinear optical effect governed by the electric dipole moment (therefore, much more intense than the 2PA-CD) and is usually defined as $\Delta\sigma^{2PA}_{CLD}(\lambda) = [\Omega^{2PA}_{CLD}(\lambda) - 1]/[\Omega^{2PA}_{CLD}(\lambda) + 1]$, where $\Omega^{2PA}_{CLD}(\lambda) = \sigma^{2PA}_{CP}(\lambda)/\sigma^{2PA}_{LP}(\lambda)$ is the ratio between the 2PA cross-section obtained by using circularly

dx.doi.org/10.1021/jz4007004 | *J. Phys. Chem. Lett.* 2013, 4, 1753–1759

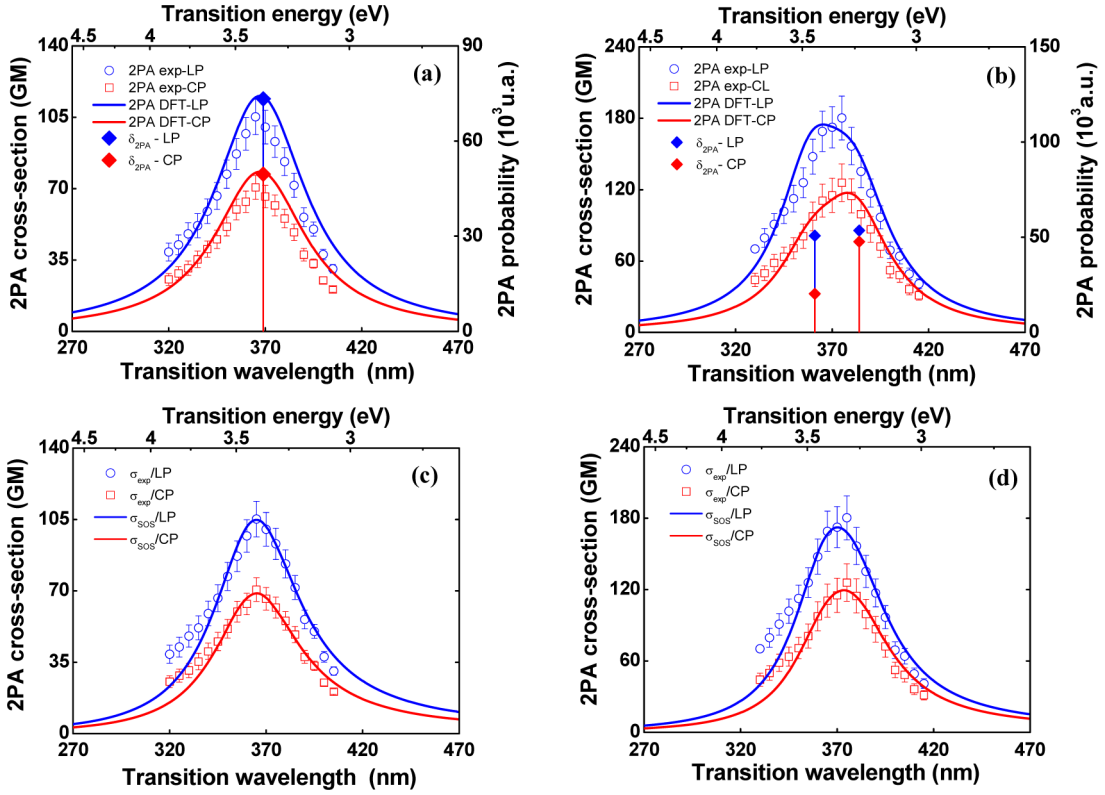

Figure 3. 2PA (circles for linear polarization and squares for circular polarization) spectra of (a) **FD43** and (b) **FD48**. In (a) and (b), the solid lines along the circles and squares correspond to simulated 2PA spectra based on the theoretical results, and the results in (c) and (d) correspond to the SOS approach. In (a) and (b), the scattered diamonds show the 2PA probability obtained from theoretical calculations for each specific transition. The theoretical spectrum in (a) is shifted by −10 nm.

($\sigma_{CP}^{2PA}(\lambda)$) and linearly ($\sigma_{LP}^{2PA}(\lambda)$) polarized lights. Because the 2PA ratio can be explicitly written in terms of the orientational average of the dipole moments' magnitude from ground and excited states, as well as its relative orientation, the 2PA-CLD technique may provide information about the electronic and molecular structures of randomly oriented chromophores. The molecular structures of the chiral π-conjugated molecules (**FD43** and **FD48**) studied are presented in Figure 1. As it is seen, **FD43** chirality arises from the chiral carbon attached to the phenyl ligand, while the chirality of **FD48** is due to the presence of chiral carbons in the cyclohexane ring bearing the substituents, which confers a helical structure to the molecule. Details about the synthesis and purification of these compounds can be found in ref 39.

To investigate the 2PA-CLD spectra, we used the wavelength-tunable femtosecond Z-scan technique and quantum chemical calculations combined with the response function formalism within the density functional theory (DFT) framework.[40,41] Experimental and theoretical details can be found in the Supporting Information.

The molar absorptivity spectra of **FD43** and **FD48** are displayed by the solid lines in Figure 2a and b, respectively. Such spectra present a lowest-energy absorption band at approximately 370 nm in the case of both molecules, with molar absorptivity of ∼3.4 and 6.4 × 10^4 mol^{-1} L cm^{-1}, respectively. The origin of this band is associated with a $\pi \rightarrow \pi^*$ transition localized in the π-conjugated phenylacetylene backbone.[39]

The circles and squares in Figures 2a and 2b show, respectively, the lowest-energy 2PA-allowed band determined by open-aperture Z-scan with linearly and circularly polarized light. A significant difference in the 2PA cross-section is found when using circularly and linearly polarized light, approximately 35 GM for **FD43** and 60 GM for **FD48**.

Such a difference is associated with elements of the 2PA tensor, which can be related to the symmetry of the electronic states, as well as to the angle between the dipole moments.[23,25] To gain new insights into the electronic and molecular structures of **FD43** and **FD48**, we show the experimental (diamonds) and simulated (solid lines) 2PA-CLD spectra, respectively, in Figures 2c and 2d.

The first aspect to be highlighted, based on the analysis of the data present in Figures 2c and 2d, is the good agreement between the simulated and experimental 2PA-CLD spectra. The theory clearly reproduces the constant behavior observed for **FD43** (Figure 2c), with $\Omega_{CLD} \approx 0.68$, as well as the sigmoidal behavior for **FD48** (Figure 2d).

From the trend observed in Figure 2d, we discriminate two regions in which Ω_{CLD} tends to constant values; the first one, between approximately 380 and 420 nm, has $\langle\Omega_{CLD}\rangle \approx 0.76$, and the other one, between 330 and 360 nm, has $\langle\Omega_{CLD}\rangle \approx 0.62$. These results suggest that the 2PA bands of **FD43** and **FD48**, located at 370 nm, are ascribed to one and two (at least) strongly 2PA-allowed states, respectively. In an attempt to verify this hypothesis, we performed quantum chemical calculations based on the DFT framework. The solid lines along the experimental data (circles and squares) in Figures 3a and 3b display the simulated spectra using the results provided by the quadratic response function calculation.[40,41]

dx.doi.org/10.1021/jz4007004 | J. Phys. Chem. Lett. 2013, 4, 1753−1759

The theoretical results indicate the existence of respectively one and two electronic states with high 2PA probability in that spectral region in the case of **FD43** ($\overline{\delta}^{2PA}_{S_0\rightarrow S_1}$ = 73300 au (97 GM)) and **FD48** ($\overline{\delta}^{2PA}_{S_0\rightarrow S_1}$ = 53500 au (102 GM); $\overline{\delta}^{2PA}_{S_0\rightarrow S_2}$ = 50800 au (110 GM)) molecules (see scattered diamonds in Figures 3a and 3b). Therefore, the results provided by the quantum chemical calculations corroborate the interpretation obtained from the analysis of Figure 2c and d. In addition, in the case of **FD48**, the theoretical calculations show that the two states lie very closely; in fact, the energy separation is approximately 0.2 eV, in agreement with the experimental results presented in Figure 2d. Moreover, it is worth mentioning that the 2PA spectrum for FD48 presents a small red shift as compared to its 1PA spectrum. Such behavior can be explained, according to the theoretical calculations, because the 1PA oscillator strength of the second excited state is considerably higher than the first excited state (f_{S1}= 1.09 at 384 nm and f_{S2} = 1.48 at 361 nm), while for the 2PA cross-section, the opposite is observed, that is, the first excited state presents higher 2PA probability ($\overline{\delta}^{2PA}_{S_0\rightarrow S_1}$ = 53500 au) as compared with the second excited state ($\overline{\delta}^{2PA}_{S_0\rightarrow S_2}$ = 50800 au). Such behavior produces as a final result a small red shift (70 meV) in the 2PA spectrum as compared to the 1PA spectrum. The experimental results endorse such an observation; in fact, there are two excited state strongly allowed by 2PA close to each another.

Another interesting aspect observed in Figures 2c and 2d is that the 2PA-CLD spectra, simulated and experimental, only exhibit negative values ($\Delta\sigma^{2PA}_{CLD} < 0$) within the investigated spectral range. These results point out that the excited states, responsible for the 2PA-allowed band, have the same symmetry as the ground state.[23] However, as **FD43** and **FD48** do not have inversion of symmetry, it is not expected that the excited states present a well-defined symmetry and, therefore, the dipole-electric selection rules are most probably relaxed.[42] In this situation, it is not possible to guarantee the symmetry of the excited states of both molecules. Although **FD43** and **FD48** have molecular chirality, as previously mentioned, we did not observe, within our experimental error, differences between 2PA cross-sections measured using right and left circularly polarized light (this result can be seen in the Supporting Information).

In order to support our results and their interpretations, as well as to establish a relationship between the 2PA-CLD spectrum and the electronic/molecular structure of the compounds, we used the sum-over-essential states (SOS) approach. In doing so, we considered the energy levels obtained from the quantum chemical calculations. Proceeding in this way, we used a two-energy level diagram for **FD43** and a three-energy level diagram with two final states for **FD48** (see the Supporting Information) because this molecule has two strongly 2PA-allowed excited states with virtually the same probability.[39] For **FD43**, within the two-energy level approximation, the 2PA-CLD signal can be written as (see the Supporting Information)[33,38]

$$\Omega^{2PA}_{CLD} = \left\{\frac{\cos^2(\theta_{\vec{\mu}_{01}\Delta\vec{\mu}_{01}}) + 3}{2[2\cos^2(\theta_{\vec{\mu}_{01}\Delta\vec{\mu}_{01}}) + 1]}\right\} \quad (1)$$

where θ is the angle between the dipole moments $\vec{\mu}_{01}$ and $\Delta\vec{\mu}_{01}$. It is observed that in a two-level system, Ω^{2PA}_{CLD} varies between 0.667 ($\theta\vec{\mu}_{01}\Delta\vec{\mu}_{01}$ = 0°) and 1.5 ($\theta\vec{\mu}_{01}\Delta\vec{\mu}_{01}$ = 90°) for any value of the angle between the dipole moments and does not present any dependence on the wavelength. In Figure 2c, the dashed line shows the fit obtained employing eq 1 with $\theta_{\vec{\mu}_{01}\Delta\vec{\mu}_{01}}$ = 8° ± 4°. Such result is in good agreement with the one obtained from the response function calculations ($\theta_{\vec{\mu}_{01}\Delta\vec{\mu}_{01}}$ = 11.5°, solid line in Figure 2c). Furthermore, as can be noted based on the analysis of Figure 4a, the π-conjugated bridge and the electron donor and acceptor groups are in the same plane for **FD43** and, therefore, it is expected that the dipole moments are virtually parallel, corroborating the small value obtained for $\theta_{\vec{\mu}_{01}\Delta\vec{\mu}_{01}}$. In addition, as can be seen in Figure 3c (solid lines), the $\theta_{\vec{\mu}_{01}\Delta\vec{\mu}_{01}}$ value reproduces well, within the SOS approach, the experimental 2PA spectra measured with linearly and circularly polarized light.

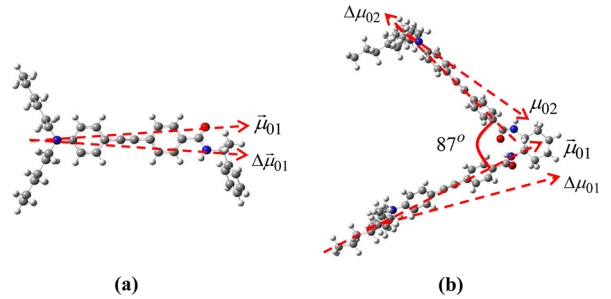

Figure 4. Equilibrium molecular geometry of (a) **FD43** and (b) **FD48**. The arrows display the direction of the dipole moments obtained by the combined polarized Z-scan technique and theoretical results.

Because, according to the theoretical calculations, **FD48** presents two 2PA-allowed transitions very close in energy and with similar probabilities, it is necessary to consider a three-energy level diagram with two final states. In this system, the Ω^{2PA}_{CLD} signal can be written as (see the Supporting Information)

$$\Omega^{2PA}_{CLD}(\omega) = \frac{\sigma^{2PA}_{CP}}{\sigma^{2PA}_{LP}} = \frac{\alpha\eta g_{01}(2\omega) + \left[\beta\kappa + R(\omega)\chi\rho + 2R(\omega)\gamma\frac{(\omega_{01}-\omega)}{\omega}\varsigma\right]g_{02}(2\omega)}{\alpha\tau g_{01}(2\omega) + \left[\beta\psi + R(\omega)\chi\zeta + 2R(\omega)\gamma\frac{(\omega_{01}-\omega)}{\omega}\vartheta\right]g_{02}(2\omega)} \quad (2)$$

where $R(\omega) = \omega^2/[(\omega_{01}-\omega)^2 + \Gamma^2_{01}(\omega)]$ is the 2PA resonance enhancement factor, $g(2\omega)$ is the line shape function, and ω is the excitation frequency. The parameters associated with the angle between the dipole moments are given by

$$\eta = 2[2\cos^2(\theta_{\vec{\mu}_{01}\Delta\vec{\mu}_{01}}) + 1] \quad (2a)$$

$$\kappa = 2[2\cos^2(\theta_{\vec{\mu}_{02}\Delta\vec{\mu}_{02}}) + 1] \quad (2b)$$

$$\rho = 2[2\cos^2(\theta_{\vec{\mu}_{01}\vec{\mu}_{12}}) + 1] \quad (2c)$$

$$\varsigma = 2\left[\cos(\theta_{\vec{\mu}_{02}\Delta\vec{\mu}_{02}})\cos(\theta_{\vec{\mu}_{01}\vec{\mu}_{12}}) + \cos(\theta_{\vec{\mu}_{12}\Delta\vec{\mu}_{02}})\cos(\theta_{\vec{\mu}_{01}\vec{\mu}_{02}}) + \cos(\theta_{\vec{\mu}_{01}\Delta\vec{\mu}_{02}})\cos(\theta_{\vec{\mu}_{02}\vec{\mu}_{12}})\right] \quad (2d)$$

for linear polarization and

$$\tau = [\cos^2(\theta_{\vec{\mu}_{01}\Delta\vec{\mu}_{01}}) + 3] \quad (2e)$$

dx.doi.org/10.1021/jz4007004 | J. Phys. Chem. Lett. 2013, 4, 1753−1759

$$\psi = [\cos^2(\theta_{\vec{\mu}_{02}\Delta\vec{\mu}_{02}}) + 3] \quad (2f)$$

$$\zeta = [\cos^2(\theta_{\vec{\mu}_{01}\vec{\mu}_{12}}) + 3] \quad (2g)$$

$$\vartheta = \left[-2\cos(\theta_{\vec{\mu}_{02}\Delta\vec{\mu}_{02}})\cos(\theta_{\vec{\mu}_{01}\vec{\mu}_{12}}) + 3\cos(\theta_{\vec{\mu}_{12}\Delta\vec{\mu}_{02}})\cos(\theta_{\vec{\mu}_{01}\vec{\mu}_{02}}) + 3\cos(\theta_{\vec{\mu}_{01}\Delta\vec{\mu}_{02}})\cos(\theta_{\vec{\mu}_{02}\vec{\mu}_{12}})\right] \quad (2h)$$

for circular polarization.

The other parameters $\alpha = |\vec{\mu}_{01}|^2|\Delta\vec{\mu}_{01}|^2$, $\beta = |\vec{\mu}_{02}|^2|\Delta\vec{\mu}_{02}|^2$, $\chi = |\vec{\mu}_{01}|^2|\vec{\mu}_{12}|^2$, and $\gamma = |\vec{\mu}_{01}||\vec{\mu}_{12}||\vec{\mu}_{02}||\Delta\vec{\mu}_{02}|$, shown in Table 1, are associated with the magnitude of the dipole moments. Such parameters can be obtained through solvatochromic shift measurements, as reported in ref 39.

Table 1. Parameters Associated with the Magnitude of the Dipole Moments

parameters (Debye[4])	DFT	SOS
α	16630	15190
β	17095	9950
χ	187	163
γ	1788	1372

It is very challenging to obtain the angle between the dipole moments directly from the experimental data due to the large number of parameters involved in eq 2. In this Letter, however, an attempt to estimate the angles was made using the results provided by the theoretical calculations. Subsequently, to obtain the angle between the dipole moments from the experimental data, we fit the experimental 2PA-CLD spectrum (dashed line in Figure 2d and solid lines in Figure 3d) using the least-squares-based finite difference method,[43] taking as the initial values those obtained through the theoretical calculations. Table 2 shows the values estimated through the two approaches. It is observed that, in general, there are good agreements between the values provided by both. The values estimated for the parameter β (Table 1) and the angle between the dipole moments $\vec{\mu}_{01}$ and $\Delta\vec{\mu}_{01}$ (Table 2) are the only exceptions because for those, a considerable difference is observed. These parameters, to some extent, may explain the difference between the experimental and theoretical data verified in Figure 2d for the spectral region below 360 nm. Figure 4b shows the equilibrium molecular geometry for **FD48**, with the arrows illustrating the direction of the dipole moments obtained from the experimental data and theoretical results (Table 2).

Table 2. Estimates of the Angles between the Dipole Moments of the FD48 Molecule[a]

dipole angles	DFT (deg)	SOS (deg)
$\theta_{\vec{\mu}_{01}\Delta\vec{\mu}_{01}}$	18	45
$\theta_{\vec{\mu}_{02}\Delta\vec{\mu}_{02}}$	172	180
$\theta_{\vec{\mu}_{01}\vec{\mu}_{02}}$	101	91
$\theta_{\vec{\mu}_{01}\vec{\mu}_{12}}$	151	155
$\theta_{\vec{\mu}_{01}\Delta\vec{\mu}_{02}}$	87	85
$\theta_{\vec{\mu}_{02}\vec{\mu}_{12}}$	64	80
$\theta_{\vec{\mu}_{12}\Delta\vec{\mu}_{02}}$	108	118

[a]The estimates were made based on the theoretical results (DFT) and by modeling the experimental 2PA-CLD spectrum using the SOS approach.

The result indicates that the angle between the two branches is equal to the angle between the transition dipole moment $\vec{\mu}_{01}$ and $\vec{\mu}_{02}$, and therefore, it suggests that each branch of **FD48** is responsible for one of its strongly 2PA-allowed states. Another important aspect to be highlighted in Figure 4b is that the angle between the two branches is approximately 90°. Such an angle ensure a basically null contribution from the interference term (third term of the numerator and denominator in brackets in eq 2) between the two distinct excitation pathways present in a three-energy level system (see the Supporting Information) because, in the SOS approach, the interference term depends directly on $\cos(\theta)$, where θ is the angle between the dipole moments along each branch (indices 1 and 2). For the two distinct excitation pathways, one involves a transition in a three-energy level system via intermediate one-photon resonance (second term of the numerator and denominator in brackets in eq 2), and the other (first term of the numerator and denominator in brackets in eq 2) connects the same initial and final states but does not involve an intermediate level because of appreciable change of the permanent dipole moment upon excitation. Depending on the relative orientation between the dipole moments, the contribution of the interference term for the 2PA can substantially increase or decrease its cross-section. We have calculated this contribution and, although it is a constructive interference process,[44] it is responsible for less than 5% of the total 2PA cross-section of the lowest-energy 2PA-allowed band for the **FD48**. Analysis of the interference channel reveals that the molecular structure of **FD48** can be tuned to increase considerably the 2PA strength.

In summary, we have interpreted the electronic and molecular structure of two molecules with different molecular structures (linear for **FD43** and V-shape for **FD48**) using the polarization-resolved femtosecond Z-scan technique and quantum chemical calculations. By using the appropriate energy diagram within the SOS approach and the response function calculations, we have modeled the 2PA-CLD spectrum and interpreted photophysical parameters with regard to the electronic and molecular structure of two randomly oriented chiral chromophores. We have observed a strong correlation between the experimental data and theoretical results for the magnitude, spectral behavior and photophysical parameters involved in the 2PA-CLD process. Finally, we have shown that the V-shape molecular geometry of the **FD48** chromophore produces a small contribution to the quantum-interference-modulated 2PA strength.

■ ASSOCIATED CONTENT

Supporting Information

Details about the two-photon experimental setup, electronic CD spectra, theoretical approach about the 2PA-CLD and a description of the sum-over-essential states approach used to interpret the results of two-photon circular and circular−linear dichroism are reported. This material is available free of charge via the Internet at http://pubs.acs.org.

■ AUTHOR INFORMATION

Corresponding Author

*E-mail: crmendonca@ifsc.usp.br (C.R.M.); mavivas82@yahoo.com.br (M.G.V.).

Notes

The authors declare no competing financial interest.

■ ACKNOWLEDGMENTS

Financial support from FAPESP (Fundação de Amparo à Pesquisa do estado de São Paulo), CNPq (Conselho Nacional de Desenvolvimento Científico e Tecnológico), Coordenação de Aperfeiçoamento de Pessoal de Nível Superior (CAPES), and the Air Force Office of Scientific Research (FA9550-12-1-0028) are acknowledged. The authors also gratefully acknowledge the allotment of the CPU time in the Wrocław Center of Networking and Supercomputing (WCSS). One of the authors (R.Z.) is the beneficiary of the KOLUMB fellowship funded by the Foundation for Polish Science (FNP).

■ REFERENCES

(1) Chung, S. J.; Zheng, S. J.; Odani, T.; Beverina, L.; Fu, J.; Padilha, L. A.; Biesso, A.; Hales, J. M.; Zhan, X. W.; Schmidt, K.; Ye, A. J.; Zojer, E.; Barlow, S.; et al. Extended Squaraine Dyes with Large Two-Photon Absorption Cross-Sections. *J. Am. Chem. Soc.* **2006**, *128*, 14444−14445.

(2) Correa, D. S.; De Boni, L.; Balogh, D. T.; Mendonca, C. R. Three- and Four-Photon Excitation of Poly(2-methoxy-5-(2′-ethyl-hexyloxy)-1,4-phenylenevinylene) (MEH-PPV). *Adv. Mater.* **2007**, *19*, 2653−2656.

(3) Cumpston, B. H.; Ananthavel, S. P.; Barlow, S.; Dyer, D. L.; Ehrlich, J. E.; Erskine, L. L.; Heikal, A. A.; Kuebler, S. M.; Lee, I. Y. S.; Mccord-Maughon, D.; et al. Two-Photon Polymerization Initiators for Three-Dimensional Optical Data Storage and Microfabrication. *Nature* **1999**, *398*, 51−54.

(4) Denk, W.; Strickler, J. H.; Webb, W. W. Two-Photon Laser Scanning Fluorescence Microscopy. *Science* **1990**, *248*, 73−76.

(5) Drobizhev, M.; Hughes, T. E.; Stepanenko, Y.; Wnuk, P.; O'Donnell, K.; Scott, J. N.; Callis, P. R.; Mikhaylov, A.; Dokken, L.; Rebane, A. Primary Role of the Chromophore Bond Length Alternation in Reversible Photoconversion of Red Fluorescence Proteins. *Sci. Rep.* **2012**, *2*, 1.

(6) Drobizhev, M.; Makarov, N. S.; Tillo, S. E.; Hughes, T. E.; Rebane, A. Two-Photon Absorption Properties of Fluorescent Proteins. *Nat. Methods* **2011**, *8*, 393−399.

(7) Gao, D.; Agayan, R. R.; Xu, H.; Philbert, M. A.; Kopelman, R. Nanoparticles for Two-Photon Photodynamic Therapy in Living Cells. *Nano Lett.* **2006**, *6*, 2383−2386.

(8) Hales, J. M.; Matichak, J.; Barlow, S.; Ohira, S.; Yesudas, K.; Bredas, J. L.; Perry, J. W.; Marder, S. R. Design of Polymethine Dyes with Large Third-Order Optical Nonlinearities and Loss Figures of Merit. *Science* **2010**, *327*, 1485−1488.

(9) He, G. S.; Tan, L. S.; Zheng, Q.; Prasad, P. N. Multiphoton Absorbing Materials: Molecular Designs, Characterizations, and Applications. *Chem. Rev.* **2008**, *108*, 1245−1330.

(10) Hu, H.; Fishman, D. A.; Gerasov, A. O.; Przhonska, O. V.; Webster, S.; Padilha, L. A.; Peceli, D.; Shandura, M.; Kovtun, Y. P.; Kachkovski.; et al. Two-Photon Absorption Spectrum of a Single Crystal Cyanine-Like Dye. *J. Phys. Chem. Lett.* **2012**, *3*, 1222−1228.

(11) Kawata, S.; Kawata, Y. Three-Dimensional Optical Data Storage Using Photochromic Materials. *Chem. Rev.* **2000**, *100*, 1777−1788.

(12) Kawata, S.; Sun, H. B.; Tanaka, T.; Takada, K. Finer Features for Functional Microdevices — Micromachines can be Created with Higher Resolution Using Two-Photon Absorption. *Nature* **2001**, *412*, 697−698.

(13) Marder, S. R.; Gorman, C. B.; Meyers, F.; Perry, J. W.; Bourhill, G.; Bredas, J. L.; Pierce, B. M. A Unified Description of Linear and Nonlinear Polarization in Organic Polymethine Dyes. *Science* **1994**, *265*, 632−635.

(14) Marder, S. R.; Perry, J. W.; Bourhill, G.; Gorman, C. B.; Tiemann, B. G.; Mansour, K. Relation Between Bond-Length Alternation and 2nd Electronic Hyperpolarizability of Conjugated Organic-Molecules. *Science* **1993**, *261*, 186−189.

(15) Parthenopoulos, D. A.; Rentzepis, P. M. 3D Optical Storage Memory. *Science* **1989**, *245*, 843−845.

(16) Perry, J. W.; Mansour, K.; Lee, I. Y. S.; Wu, X. L.; Bedworth, P. V.; Chen, C. T.; Ng, D.; Marder, S. R.; Miles, P.; Wada, T.; et al. Organic Optical Limiter with a Strong Nonlinear Absorptive Response. *Science* **1996**, *273*, 1533−1536.

(17) Vivas, M. G.; Mendonca, C. R. Temperature Effect on the Two-Photon Absorption Spectrum of All-*trans*-β-Carotene. *J. Phys. Chem. A* **2012**, *116*, 7033−7038.

(18) Zhu, X.; Kao, Y.-T.; Min, W. Molecular-Switch-Mediated Multiphoton Fluorescence Microscopy with High-Order Nonlinearity. *J. Phys. Chem. Lett.* **2012**, *3*, 2082−2086.

(19) Goeppert-Mayer, M. On Elementary Acts with Two Quantum Jumps. *Ann. Phys.* **1931**, *8*, 273−294.

(20) Orr, B. J.; Ward, J. F. Perturbation Theory of Non-Linear Optical Polarization of an Isolated System. *Mol. Phys.* **1971**, *20*, 513−526.

(21) Toro, C.; De Boni, L.; Lin, N.; Santoro, F.; Rizzo, A.; Hernandez, F. E. Two-Photon Absorption Circular−Linear Dichroism on Axial Enantiomers. *Chirality* **2010**, *22*, E202−E210.

(22) Vivas, M. G.; De Boni, L.; Bretonniere, Y.; Andraud, C.; Mendonca, C. R. Polarization Effect on the Two-Photon Absorption of a Chiral Compound. *Opt. Express* **2012**, *20*, 18600−18608.

(23) Nascimento, M. A. C. The Polarization Dependence of 2-Photon Absorption Rates for Randomly Oriented Molecules. *Chem. Phys.* **1983**, *74*, 51−66.

(24) Theisen, M.; Linke, M.; Kerbs, M.; Fidder, H.; Madjet, M. E. A.; Zacarias, A.; Heyne, K. Femtosecond Polarization Resolved Spectroscopy: A Tool for Determination of the Three-Dimensional Orientation of Electronic Transition Dipole Moments and Identification of Configurational Isomers. *J. Chem. Phys.* **2009**, *131*, 124511.

(25) Tinoco, I. Two-Photon Circular Dichroism. *J. Chem. Phys.* **1975**, *62*, 1006−1009.

(26) Toro, C.; De Boni, L.; Lin, N.; Santoro, F.; Rizzo, A.; Hernandez, F. E. Two-Photon Absorption Circular Dichroism: A New Twist in Nonlinear Spectroscopy. *Chem.—Eur. J.* **2010**, *16*, 3504−3509.

(27) Mcclain, W. M. Excited State Symmetry Assignment through Polarized 2-Photon Absorption Studies of Fluids. *J. Chem. Phys.* **1971**, *55*, 2789−2796.

(28) Power, E. A. Two-Photon Circular Dichroism. *J. Chem. Phys.* **1975**, *63*, 1348−1350.

(29) Wanapun, D.; Wampler, R. D.; Begue, N. J.; Simpson, G. J. Polarization-Dependent Two-Photon Absorption for the Determination of Protein Secondary Structure: A Theoretical Study. *Chem. Phys. Lett.* **2008**, *455*, 6−12.

(30) Olesiak-Banska, J.; Mojzisova, H.; Chauvat, D.; Zielinski, M.; Matczyszyn, K.; Tauc, P.; Zyss, J. Liquid Crystal Phases Of DNA: Evaluation of DNA Organization by Two-Photon Fluorescence Microscopy and Polarization Analysis. *Biopolymers* **2011**, *95*, 365−375.

(31) Mojzisova, H.; Olesiak, J.; Zielinski, M.; Matczyszyn, K.; Chauvat, D.; Zyss, J. Polarization-Sensitive Two-Photon Microscopy Study of the Organization of Liquid-Crystalline DNA. *Biophys. J.* **2009**, *97*, 2348−2357.

(32) Diaz, C.; Lin, N.; Toro, C.; Passier, R.; Rizzo, A.; Hernandez, F. E. The Effect of the π-Electron Delocalization Curvature on the Two-Photon Circular Dichroism of Molecules with Axial Chirality. *J. Phys. Chem. Lett.* **2012**, *3*, 1808−1813.

(33) Meath, W. J.; Power, E. A. On the Importance of Permanent Moments in Multiphoton Absorption using Perturbation-Theory. *J. Phys. B: At., Mol. Opt. Phys.* **1984**, *17*, 763−781.

(34) Andrews, D. L.; Thirunamachandran, T. On Three-Dimensional Rotational Averages. *J. Chem. Phys.* **1977**, *67*, 5026.

(35) Vivas, M. G.; Dias, C.; Echevarría, L.; Mendonca, C. R.; Hernandez, F. E.; De Boni, L. Two-Photon Circular−Linear Dichroism of Perylene in Solution: A Theoretical−Experimental Study. *J. Phys. Chem. B* **2013**, *117*, 2742−2747.

(36) Meath, W. J.; Power, E. A. Differential Multiphoton Absorption by Chiral Molecules and the Effect of Permanent Moments. *J. Phys. B: At., Mol. Opt. Phys.* **1987**, *20*, 1945−1964.
(37) Fischer, P.; Hache, F. Nonlinear Optical Spectroscopy of Chiral Molecules. *Chirality* **2005**, *17*, 421−437.
(38) Hoeben, F. J. M.; Jonkheijm, P.; Meijer, E. W.; Schenning, A. About Supramolecular Assemblies of π-Conjugated Systems. *Chem. Rev.* **2005**, *105*, 1491−1546.
(39) Vivas, M. G.; Silva, D. L.; De Boni, L.; Bretonniere, Y.; Andraud, C.; Laibe-Darbour, F.; Mulatier, J. C.; Zaleśny, R.; Bartkowiak, W.; Canuto, S.; et al. Experimental and Theoretical Study on the One- and Two-Photon Absorption Properties of Novel Organic Molecules Based on Phenylacetylene and Azoaromatic Moieties. *J. Phys. Chem. B* **2012**, *116*, 14677−14688.
(40) Salek, P.; Vahtras, O.; Helgaker, T.; Agren, H. Density-Functional Theory of Linear and Nonlinear Time-Dependent Molecular Properties. *J. Chem. Phys.* **2002**, *117*, 9630−9645.
(41) Salek, P.; Vahtras, O.; Guo, J. D.; Luo, Y.; Helgaker, T.; Agren, H. Calculations of Two-Photon Absorption Cross Sections by Means of Density-Functional Theory. *Chem. Phys. Lett.* **2003**, *374*, 446−452.
(42) Bonin, K. D.; Mcilrath, T. J. Two-Photon Electric-Dipole Selection Rules. *J. Opt. Soc. Am. B* **1984**, *1*, 52−55.
(43) Nielsen, K. L. *Methods in Numerical Analysis*; Macmillan: New York, 1966.
(44) Drobizhev, M.; Meng, F. Q.; Rebane, A.; Stepanenko, Y.; Nickel, E.; Spangler, C. W. Strong Two-Photon Absorption in new Asymmetrically Substituted Porphyrins: Interference Between Charge-Transfer and Intermediate-Resonance Pathways. *J. Phys. Chem. B* **2006**, *110*, 9802−9814.